Theory of Liquid-Crystalline (LC) Polymer Brushes: Interpenetrating Brushes

Victor M. Amoskov, Tatiana M. Birshtein,* and Victor A. Pryamitsyn

Institute of Macromolecular Compounds, Academy of Sciences of Russia, 31, Bolshoy pr., St.-Petersburg, 199004, Russia

Received July 2, 1997; Revised Manuscript Received February 10, 1998

ABSTRACT: Interaction of brushes oriented face-to-face under compression and subsequent extension is investigated theoretically. Brushes formed by mesogenic chains with induced stiffness in the liquid-crystalline (LC) state are considered. It is shown that the contact between LC brushes composed of long folds of grafted chains (FLC structure) leads to interpenetration of brushes and to formation of a combined structure. The brushes remain combined under the extension of this structure.

1. Introduction

This paper continues a paper[1] (see also refs 2 and 3) devoted to a theoretical study of liquid-crystalline (LC) ordering in planar polymer brushes formed by macromolecules with mesogenic groups in the main chains. The properties of polymer brushes and brushlike systems have been attracting considerable attention for the last two decades (see review[4] and references in ref 1). Advances in statistical theory, computer simulations, and experimental studies have made it possible to understand the behavior of polymer brushes in some detail. Nevertheless, as we have already mentioned in ref 1, they continue to be an inexhaustible object of investigation, demonstrating a considerable variety of properties.

In this paper we investigate the thermodynamics and conformational rearrangements of chains under changes of the distance between two LC brushes placed in a solvent and oriented face to face. It will be shown that in drastic contrast to the typical situation[5] there is strong interpenetration of opposite brushes provided they have a folded LC structure. Moreover, the results of our investigation suggest that, due to interpenetration, the brushes appear to be glued together and remain joined even if the grafting surfaces are forced apart. The microphase-segregated metastable state of stretched LC brushes is found to be typical for such a system.

2. Model, Method, and Notation

The model and the essentials of the method of investigation are the same as in refs 1 and 3. The only difference is the consideration of two planar brushes in a solvent oriented face to face (Figure 1), instead of one brush. Let us take a brief look at the model and the method. For a more extended consideration, see the previous paper.[1]

We construct an equilibrium theory in the self-consistent field (SCF) approximation. The dimensionless free energy F of the system is (we use kT as the unit energy)

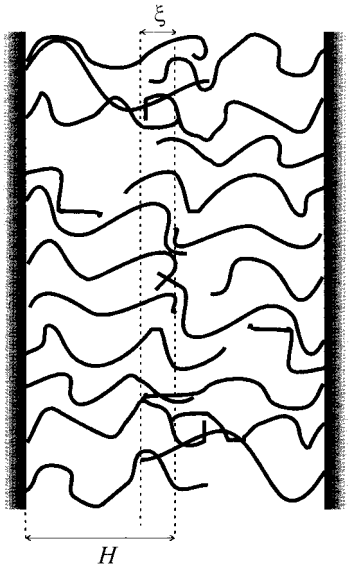

Figure 1. Outline of two planar brushes in a solvent oriented face to face.

$$F[\{\rho\}] = \int f_{\text{int}}[\rho(x)]\,\mathrm{d}x - S[\{\rho\}] \qquad (1)$$

where $\rho(x)$ is the density of segments in the layer x (the x direction is perpendicular to the grafting surfaces and the brushes are assumed to be homogeneous in the lateral directions), $\{\rho\}$ is the total segment density profile, f_{int} is the density of the free energy of short-range interactions, and S is the entropy of a system of noninteracting chains with the density profile $\{\rho\}$.

All the N segments of each chain, grafted with the grafting density σ, are assumed to be mesogenic ones; i.e., the energy of interaction between contacting segments depends on their mutual orientation. For the calculation of f_{int} we suggest a combination of the Flory−Huggins model for the isotropic part of the interaction[6,7] and the Mayer−Saupe expression for the anisotropic interaction.[8]

* E-mail: birshtei@macro.lgu.spb.su.

S0024-9297(97)00985-6 CCC: $15.00
Published on Web 05/13/1998

$$f_{int}[x] = (1 - \rho[x]) \ln(1 - \rho[x]) - \chi\rho^2[x] - \frac{\eta}{2}\rho^2[x]s_2{}^2[x] \quad (2)$$

where χ and η are the parameters of isotropic and anisotropic interactions between polymer segments and s_2 is the orientational order parameter of segments (with respect to the x axis).

The minimization of F leads to a set of equations for equilibrium density profile $\{\rho\}$ and other characteristics in the SCF approximation. To solve these equations, we use the Scheutjens−Fleer numerical method.[9] The necessary refinements of this method were introduced in ref 1 to analyze our complicated system. The Scheutjens−Fleer method was developed for lattice models of polymer brushes. In our case the chains are assumed to walk on a simple cubic lattice (SCL) with the statistical weights (α_t, α_g, α_b) of various local conformations for direct (trans isomer), turn (gauche isomer), and back steps, correspondingly. The lattice constant is used as the unit of length.

Both the original Scheutjens−Fleer method[9] and the modified version presented in our preceding paper[1] deal with one free brush subject to the boundary condition

$$\rho^i(x) = 0 \qquad \text{for} \qquad x < 0$$

where i = (⊙, +, ⊗) are the directions up, parallel, and down with respect to the grafting plane and $\rho^i(x)$ is the density of segments passing layer x in the i direction. Adding the second boundary condition,

$$\rho^i(x) = 0 \qquad \text{for} \qquad x > H$$

where H is some fixed distance, gave us the possibility of investigating the compression of a brush in the normal direction.[3] It is essential that the interaction of two identical oncoming brushes can also be investigated by a proper modification of the boundary conditions rather than the iteration procedure.

Let ρ_1 be the density of the one (for example, the left) brush that may be computed as in ref 1. It satisfies two boundary conditions

$$\rho_1^i(x) = 0 \qquad \text{for} \qquad x < 0 \quad \text{and} \quad x > 2H$$

when $2H$ is the distance between two grafting surfaces. To include the second brush (with density profile ρ_2), we add a third condition, that of symmetry. We suppose that the second brush is a mirror image of the first one relative to the plane $x = H$. The total density of segments in the system of two opposing brushes, ρ, is

$$\begin{cases} \rho^{\odot}(x) = \rho_1^{\odot}(x) + \rho_2^{\odot}(x) = \rho_1^{\odot}(x) + \rho_1^{\otimes}(2H - x) \\ \rho^{+}(x) = \rho_1^{+}(x) + \rho_2^{+}(x) = \rho_1^{+}(x) + \rho_1^{+}(2H - x) \\ \rho^{\otimes}(x) = \rho_1^{\otimes}(x) + \rho_2^{\otimes}(x) = \rho_1^{\otimes}(x) + \rho_1^{\odot}(2H - x) \end{cases} \quad (3)$$

This total density should be used in the iteration procedure instead of the density of one brush as in paper.[1]

As for a single brush,[1] the segment density of the layer x, $\rho[x]$, is a sum of its components:

$$\rho[x] = \rho^{\odot}(x) + \rho^{+}(x) + \rho^{\otimes}(x)$$

Using the density of one brush, we can compute the half-width of the overlapping zone, ξ, by the formula:

$$\xi^2 = \frac{\sum_{x=0}^{2H}(x - H)^2 \rho_1[x] \rho_2[x]}{\sum_{x=0}^{2H}\rho_1[x] \rho_2[x]} = \frac{\sum_x (x - H)^2 \rho_1[x] \rho_1[2H - x]}{\sum_x \rho_1[x] \rho_1[2H - x]} \quad (4)$$

All other characteristics ($s_2(x)$, $g(x)$, and so on) are computed by the formulas of ref 1.

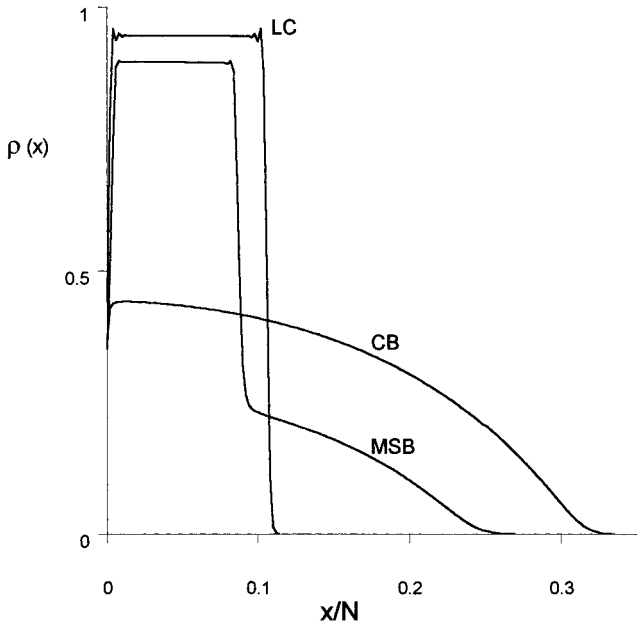

Figure 2. Outline of density profiles of a single grafted brush: CB, conventional brush, $\eta < \eta_t$; MSB, microsegregated brush, $\eta_t \le \eta < \eta_{lc}$; LC, liquid-crystalline brush, $\eta \ge \eta_{lc}$. $\rho(x)$ is the density of segments in the layer x (the x direction is perpendicular to the grafting surfaces); N is the number of segments in each polymer chain.

3. Key Features of Polymer Brushes

A. Structure of Polymer Brushes. The structure of conventional brushes (CB) formed by flexible nonmesogenic polymers is well-known.[10−12] In a good solvent ($\chi < 0.5$) they have a parabolic segment density profile. With the deterioration of solvent strength the segment density progressively increases and its value levels off through the layer.

A greater diversity of states is predicted by the theory[1−3] for brushes formed by macromolecules with anisotropic interactions between segments (Figure 2). At small values of the interaction parameter η, in the good solvent case ($\chi < 0.5$) we have the conventional brush (CB) with the parabolic density profile. With an increase in η, a phase transition to a microphase-segregated brush (MSB regime) takes place at $\eta = \eta_t$. In this regime the internal part of the brush is collapsed and orientationally ordered ($\rho \simeq 1$, $s_2 \simeq 1$); i.e., it is in the LC state, while the external sublayer is swollen. With further increases in energy η, the internal LC sublayer grows in thickness, and at sufficiently large η

$> \eta_{lc}$, this LC sublayer extends over the total height of the brush (LC state).

This qualitative picture is correct irrespective of the values of the local conformational characteristics α_t, α_g, and α_b, which affect only the values of η, corresponding to the transitions CB → MSB → LC. Nevertheless, there is a feature that depends radically on the parameters of the model. This is the mode of filling the LC layer (sublayer). It appears to be fundamentally different[1] for lattice models with and without a back-step ($\alpha_b = 1$ and $\alpha_b = 0$, or models (α_t, α_g, 1) and (α_t, α_g, 0).

If the back-step is permissible, $\alpha_b = 1$, chains move back and forth at each step inside the LC layer. If the back-step is forbidden, $\alpha_b = 0$, chains form long rigid segments packed in a folded structure inside the LC layer. This difference is related to the different physical nature of the systems: in the first case, the chains preserve their flexibility in the LC state; in the second case, LC ordering necessarily induces rigidity.

In the present paper we analyze the special features demonstrated by the LC brushes composed of chains forming the folded structure due to their induced rigidity. We will use the term *folded LC brushes* (FLC) to denote these objects. Most of the results of this paper are obtained for the model (α_t, α_g, α_b) = (110)—walks on the five-choice SCL with back-step prohibited, $\alpha_b = 0$, and $\alpha_t = \alpha_g = 1$. Other cases are presented for comparison.

B. Interaction of Brushes. Interaction of brushes, oriented as shown in Figure 1, was investigated theoretically in ref 5. Only the case of conventional brushes formed by a flexible nonmesogenic polymer was considered. It was shown that the relative thickness of the overlapping zone ξ/H (Figure 2) is very small up to strong compressions. According to the theory,[5] confirmed by numerical SCF calculations,[13] ξ/H scales as

$$\frac{\xi}{H} \sim N^{2/3}H^{-4/3} \sim N^{-2/3}\left(\frac{H_0}{H}\right)^{4/3} \qquad (5)$$

where $H_0 \sim N$ is the thickness of an undisturbed brush and $H_0/H \sim N/H$ is the degree of brush compression.

Since interpenetration of CB brushes is insignificant, the deformation of either one of the interacting brushes is similar to the deformation of a brush compressed by an impenetrable surface parallel to the grafting plane.

For brushes formed by mesogenic chains only this type of deformation has been investigated.[3] According to the theory,[3] the compression may go by diverse scenarios depending on the initial state of the undeformed brush.

The limiting cases are evident. At $\eta = 0$ (nonmesogenic chains) the layer is progressively compressed without any drastic changes. At large η, when the brush is completely in the LC state, it is practically incompressible because the solvent content is very low, $\rho \simeq 1$.

Intermediate cases are not so simple. If $\eta > \eta_t$ and the undeformed brush is in the MSB state, compression leads to a redistribution of segments between two microphases. The thickness of the internal LC sublayer increases with compression at the cost of the external CB layer.

At $0 < \eta < \eta_t$, when the undeformed brush is in the CB state, a certain degree of compression (which increases with a decrease in η) induces a phase transition from the CB to the MSB state. Further compression results in the deformation of the brush in the MSB state.

Recall that these scenarios of a deformation refer to brushes compressed by an impenetrable surface.[3] The values of local conformational characteristics of chains (α_t, α_g, α_b) do not affect the overall picture. As will be shown below, the regime of MSB deformation as well as the regime of CB deformation are both retained in the case of the brush−brush interaction. The unusual interpenetration of brushes takes place when brushes are in the FLC regime, which could be induced by a high value of η or by initial compression.

4. Overlapping and Interpenetration of FLC Brushes

Let us now proceed to the main theme of this paper, that is to the interaction of LC brushes under changes of the distance between grafting surfaces. As a measure of this distance denoted as $2H$ (see Figure 1), we use the adjusted value $H/N\sigma$ equal to the inverse average density of segments in the slit between grafting surfaces. The smallest permissible value of H corresponds to $H/N\sigma = 1$.

All the data presented below are obtained by numerical solving of the SCF equations. Except if otherwise noted, they correspond to brushes formed by chains with $N = 500$ at grafting density $\sigma = 0.1$, Flory parameter $\chi = 0.25$, and $\alpha_t = \alpha_g = 1$, $\alpha_b = 0$.

Figure 3 presents the evolution of density profiles of FLC brushes with the decrease in the distance $2H$ between grafting surfaces. The energy of anisotropic interaction η is sufficiently large ($\eta = 5$) to ensure the LC state in isolated brushes with density $\rho \sim 1$ and thickness $H/N\sigma = 1.1$, which is only slightly over the limiting value $H/N\sigma = 1$.

The density profiles of both brushes are practically undistorted until the brushes start contacting each other (Figure 3a). Even a weak contact of the brushes leads to their restructuring. At a slight compression ($H/N\sigma = 1.08$), a small fraction of segments of each brush penetrate through another brush up to the opposing grafting plane (Figure 3b). The density profiles are changed radically with future compression. At $H/N\sigma = 1.06$, the brushes penetrate each other completely to form a combined layer of two brushes "glued" together, the GB system (Figure 3c). In this GB system each brush makes a contribution $\rho \sim 0.5$ to the total density $\rho \sim 1$.

Parts a−d of Figure 4 present other brush characteristics, showing changes brought about during brush−brush interaction. For simplicity only the data for the left brush are given.

For each specific characteristic it is easy to see that the curve for combined brushes at $H/N\sigma = 1.06$ is similar to the corresponding curve for an isolated undeformed brush at $H/N\sigma = 1.1$ except that the first curve extends over the total thickness of two combined brushes in contrast to the second curve limited by the thickness of the isolated brush.

The profiles of all the characteristics of an undisturbed brush have peculiarities near the inner and outer boundaries of the layer, which are reproduced in combined brushes near the symmetrical boundaries (i.e., near the grafting surfaces). These peculiarities are two maxima of the free ends distribution (Figure 4b), a decrease in the LC order parameter s_2 (Figure 4c), and

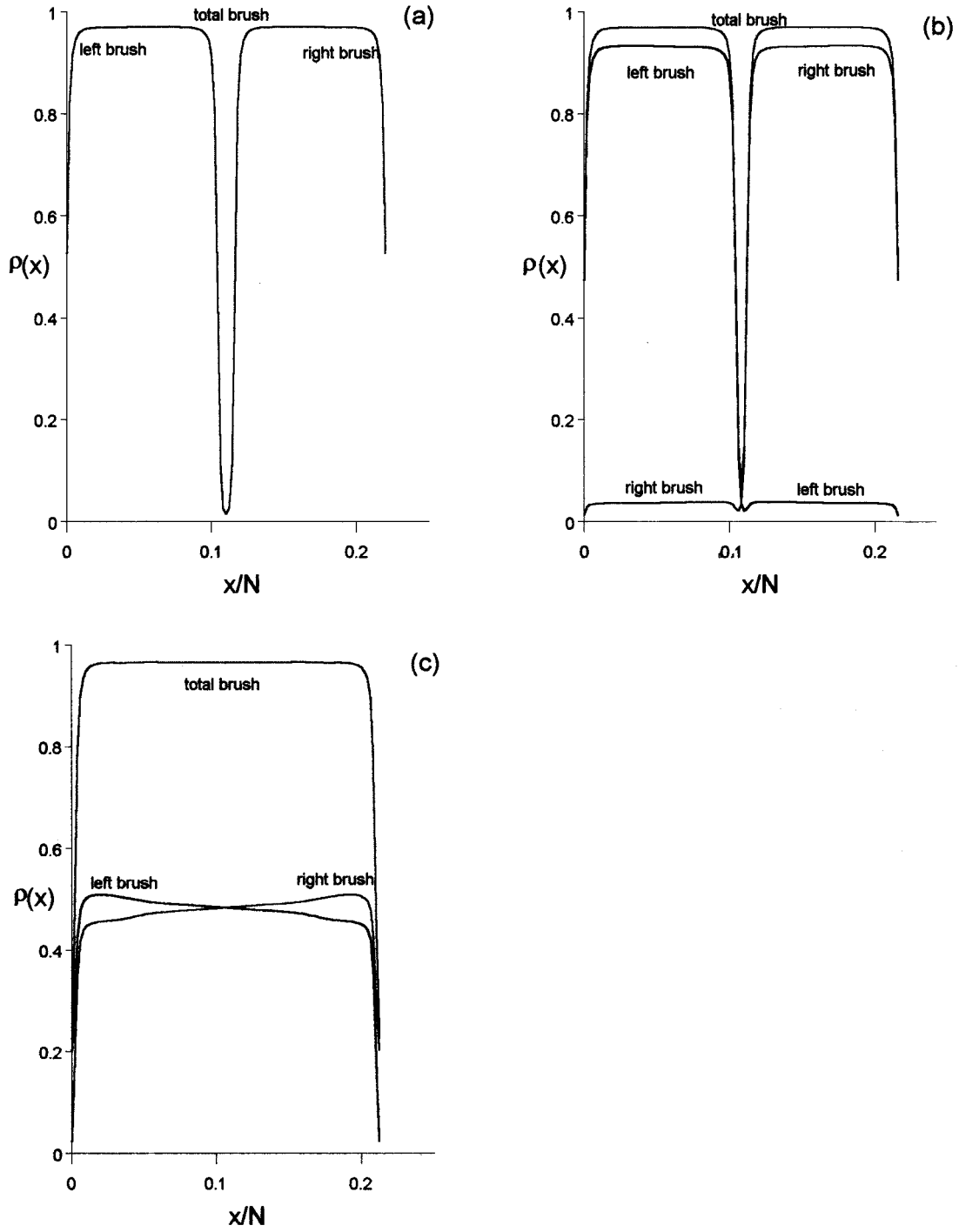

Figure 3. Evolution of density profiles of FLC brushes with the alteration of the distance $2H$ between grafting surfaces: (a) $H/N\sigma = 1.10$; (b) $H/N\sigma = 1.08$; (c) $H/N\sigma = 1.06$. $\sigma = 0.1$, $\eta = 5.0$, $\chi = 0.25$, $N = 500$, model (110).

sharp upward and downward turns of the degree of chain stretching near its own grafting surface and at the other boundary, correspondingly (Figure 4d). All these peculiarities for a single FLC brush are predominantly related to the folded structure of a brush and the fact that all defects (bends of chains, free ends) concentrate near the layer boundaries.

As follows from the data of Figures 3 and 4, in a combined GB system we also have two boundaries, but these are boundaries of the system as a whole positioned near both grafting surfaces (Figure 5). It is exactly the possibility of increasing the length of folds that is responsible for the interpenetration of FLC brushes. Note that the free end distribution of an undeformed single FLC brush has an additional (third) maximum in the middle part of a layer. This maximum is reproduced also in the combined GB system (Figure 4b). We do not have an unambiguous interpretation of the nature of this maximum even in a single brush.[1] It is possible that this is a lattice effect.

In the intermediate case at $H/N\sigma = 1.08$, where only a small fraction of segments of each brush penetrates through the other brush (Figure 3b, Figure 4a) the characteristics of a brush−brush system possess the properties of both a single brush and a combined system (Figure 4b−d). The orientational characteristics of the small fraction of guest segments appear to be nearly the same as characteristics of host segments.

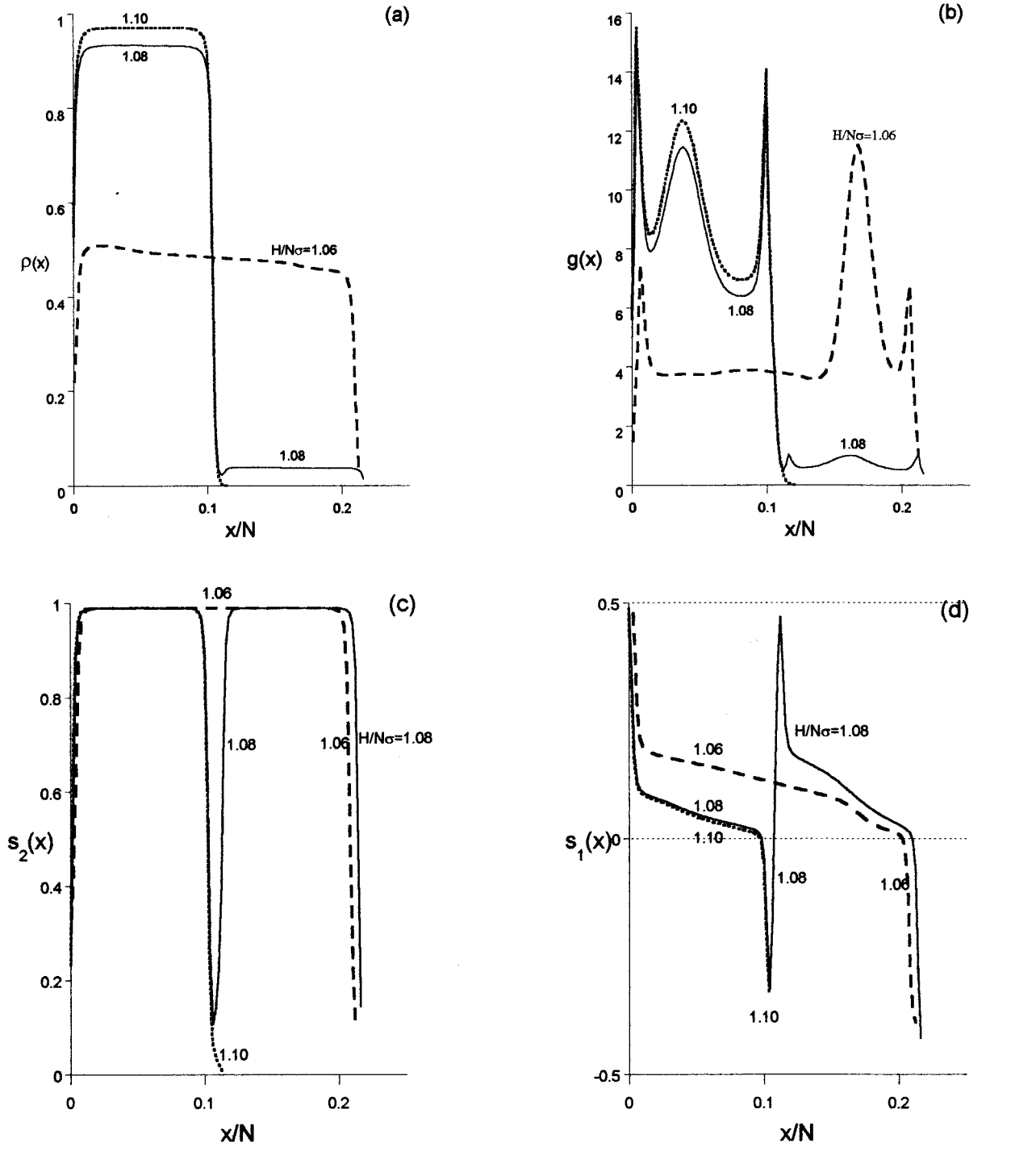

Figure 4. Profiles of several characteristics of the left brush: (a) density profiles; (b) free end distribution; (c) orientational order parameter s_2; (d) parameter of chain stretching s_1. $\sigma = 0.1$, $\eta = 5.0$, $\chi = 0.25$, $N = 500$, model (110).

Let us first illustrate the importance of an FLC structure in a brush. Figure 6 presents the density profiles and free end distribution for two interacting LC brushes formed by six-choice SCL chains (model (111)). These chains preserve their flexibility in LC brushes and do not form the FLC structure. It is seen that unlike the results presented above, compression leads to interpenetration only on the peripheries of interacting brushes. The relative thickness of the penetration zone is small: $\xi/H \ll 1$, and this zone is enriched by the free ends of both brushes. So the existence of the LC state is not sufficient to induce a complete interpenetration of chains. Interacting LC brushes formed by chains of models (110) and (111) (i.e., with and without induced rigidity correspondingly) show qualitatively different behavior.

On the contrary, when the LC arrangement is absent (parameter of anisotropic interaction η is small), the behavior of brushes in the CB state is independent of the model and is similar for models (110) and (111) (Figure 7). The decrease in H is accompanied predominantly by the compression of both brushes. The interpenetration zone ξ is small compared to H and agrees well with the scaling dependence, which may be represented by the formula

$$\frac{\xi}{N} \sim N^{-2/3}\left(\frac{H}{N}\right)^{-1/3} \qquad (6)$$

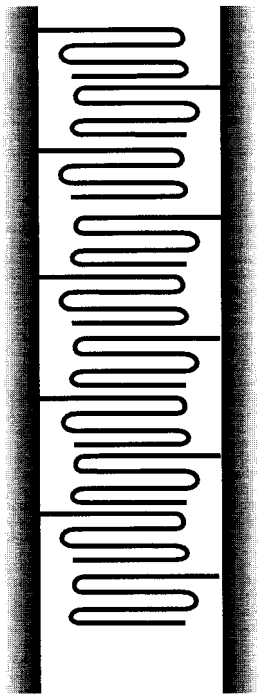

Figure 5. Outline of a combined brush−brush system.

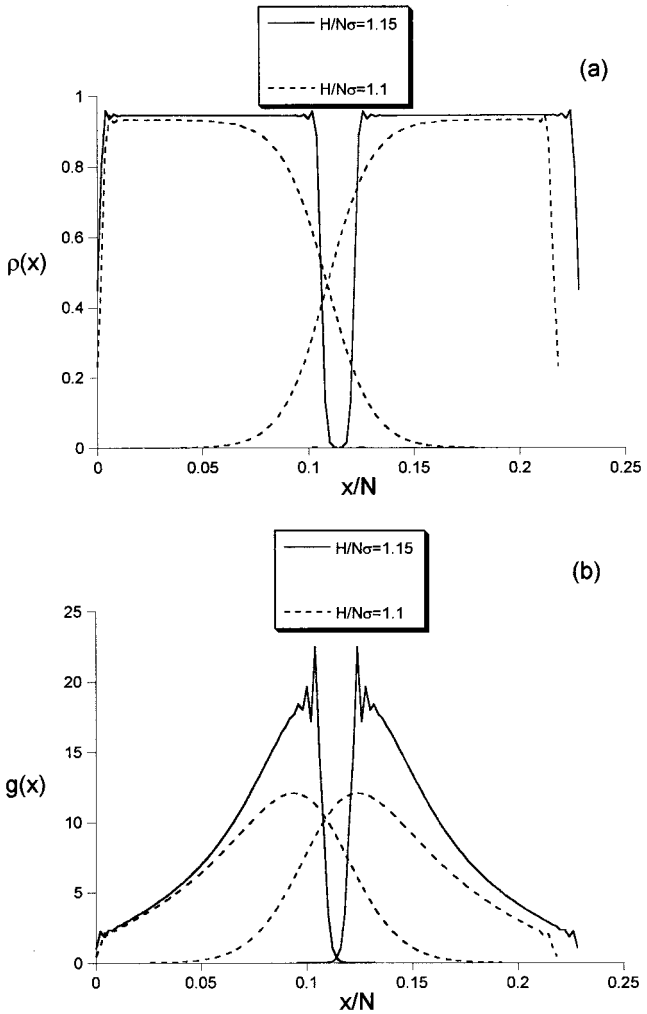

Figure 6. Density profiles (a) and free end distributions (b) of LC brushes for model (111). $\sigma = 0.1$, $\eta = 4.0$, $\chi = 0$, $N = 500$.

Figure 8 demonstrates the comparison of ξ/N to the scaling predictions $\xi/N \sim N^{-2/3}$ at fixed H/N (Figure 8a) and $\xi/N \sim (H/N)^{-1/3}$ at fixed $N = 500$ (Figure 8b). It is clear from Figure 8 that the scaling formula is correct for model (111) as well as for model (110) (and for other models too).

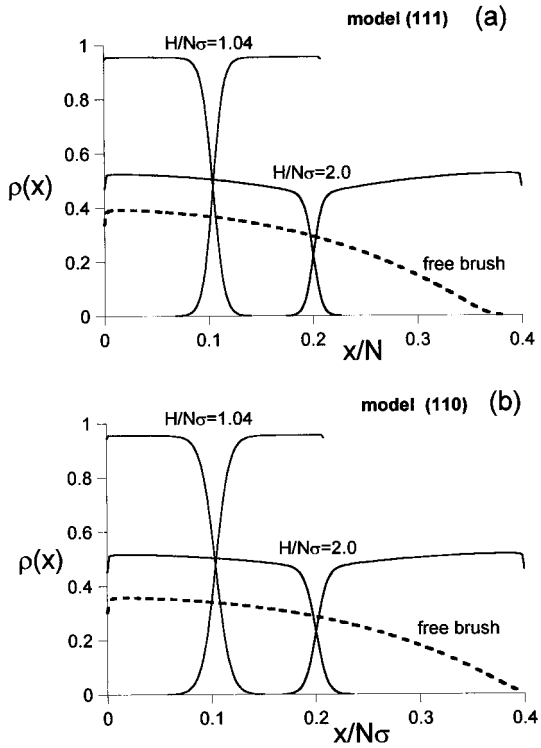

Figure 7. Density profiles of compressed brushes: (a) model (111); (b) model (110). An undisturbed single brush has been presented for comparison by a dashed line. $\sigma = 0.1$, $\chi = 0$, $\eta = 0.0$, $N = 500$.

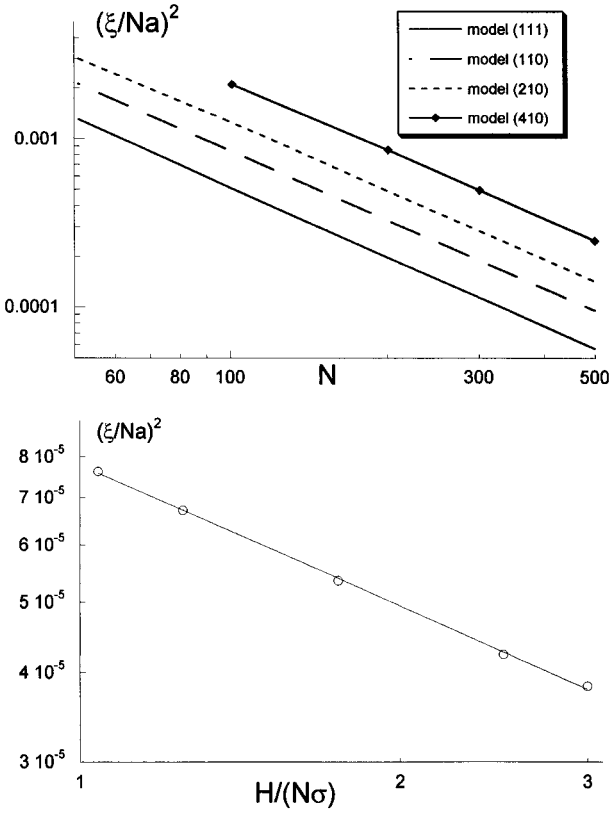

Figure 8. Scaling dependencies: (a) $(\xi/Na)^2$ vs N for fixed $H/N\sigma = 1.6$ ($\xi/N \sim N^{-0.686}$); (b) $(\xi/Na)^2$ vs $H/N\sigma$ for fixed $N = 500$, model (111) ($\xi/N \sim (H/N)^{-0.328}$). $\sigma = 0.1$, $\chi = 0$, $\eta = 0$.

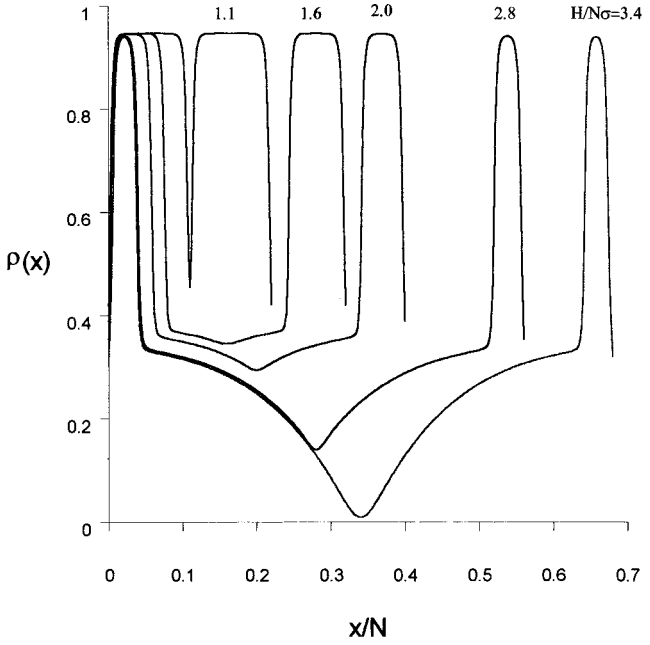

Figure 9. Profiles of total density of interacting MSB brushes. $\sigma = 0.1$, $\chi = 0.25$, $\eta = 4.15$, $N = 500$, model (110).

At the same time a preexistence of the FLC state in a single undeformed brush is not a necessary condition to form the combined GB structure. It is sufficient to have the FLC structure of a brush in a collapsed state, no matter how this state could be reached. Figure 9 presents the evolution of density profiles of interacting brushes at $\eta = 4.15$. The equilibrium state of a single undeformed brush in model (110) at $\eta = 4.15$ is the CB state with a relatively small ρ and large thickness $H/N\sigma \simeq 4$. An initial decrease in H leads to the compression of each brush and initiates the transition to the MSB state. The further decrease in H continues to lead predominantly the further compression of each brush through a redistribution of segments between microphases inside each brush. The thicknesses of internal LC sublayers increase, and the thicknesses of external CB sublayers decrease. The thickness of the interpenetration zone is small enough relative to the total brush thickness, as well as relative to the thickness of CB sublayers (Figure 10). This behavior is similar to the behavior of an MSB brush compressed by a plane parallel to the grafting surface[3] (see section 3B). It is common to all brushes in the MSB regime independent of the local conformations of chains (in particular, to the (111) and (110) models).

At compressions such that $H/N\sigma$ is close to unity, $H/N\sigma \simeq 1.1$, the external CB sublayer practically disappears and both interacting brushes attain LC structure. The behavior with further brush−brush compression depends on the model and is similar to the behavior of brushes initially in the LC state (at large η). For the (111) model with chains retaining flexibility in the LC brush, we have weakly penetrating brushes (Figure 6). For the (110) model the interpenetration of two FLC brushes gives rise to a combined GB structure. The distribution of segments at $H/N\sigma = 1.08$ and 1.06 at $\eta = 4.15$ replicates completely the distribution at $\eta = 5.0$ shown in Figure 3b,c. Note, to avoid misunderstanding, the same values $H/N\sigma = 1.1$ correspond to strong compression for initially CB brushes ($\eta = 4.15$) with $H/N\sigma \simeq 4$, in contrast to the situation for initially LC brushes (at large η) with small initial thickness $H/N\sigma \simeq 1.1$ and restricted possibility of compression.

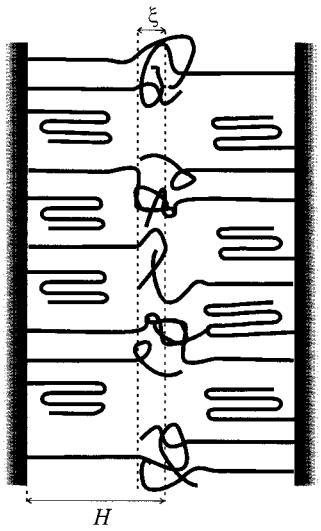

Figure 10. Outline of interacting MSB brushes with FLC sublayers.

5. Stretching of Brushes Glued Together

In the preceding section we considered the formation of the combined GB structure as a result of compressing two FLC brushes. Let us now investigate the deformation of this structure as we begin to increase the distance H between grafting surfaces.

Figure 11 presents the evolution of the density profile (a), the free end distribution (b) and the order parameter (c) with the increase in H from $H/N\sigma = 1.06$. (The evolution of this system under compression starting from two separated brushes was shown in Figure 9.) In the compressed state at $H/N\sigma = 1.06$ the brushes form the combined GB structure (Figure 5). As seen from Figure 11, according to our numerical procedure, the brushes appear to be "glued" together up to a high degree of stretching. The stretched system retains a joint FLC sublayer and forms two sublayers of stretched chains as well. In our symmetrical model (see section 2) these sublayers are arranged symmetrically and are adjacent to the grafting surfaces on each side of the combined FLC sublayer. As long as the stretching does not reach some limiting value (in this case $H/N\sigma \leq 2$), every chain passes through one of these sublayers and takes part in formation of the FLC sublayer. All the free ends reside inside the FLC sublayer. The increase in H leads only to a redistribution of segments between sublayers: the thickness of the sublayers of stretched chains increases, whereas the thickness of the FLC sublayer decreases. The other, extensive properties of sublayers (segment density ρ, order parameters s_1 and s_2) are independent of the degree of stretching. Moreover, these characteristics are practically constant along the sublayers (with the exception of the boundary effects).

This picture is typical for the behavior of a system consisting of two phases (microphases): in our stretched GB system these are a compact FLC microphase and a swollen stretched microphase.

The coexistence of compact and stretched microphases is typical under stretching of collapsed polymeric systems.[14−16] Note that in our system (brushes formed by mesogenic chains) this type of microphase separation

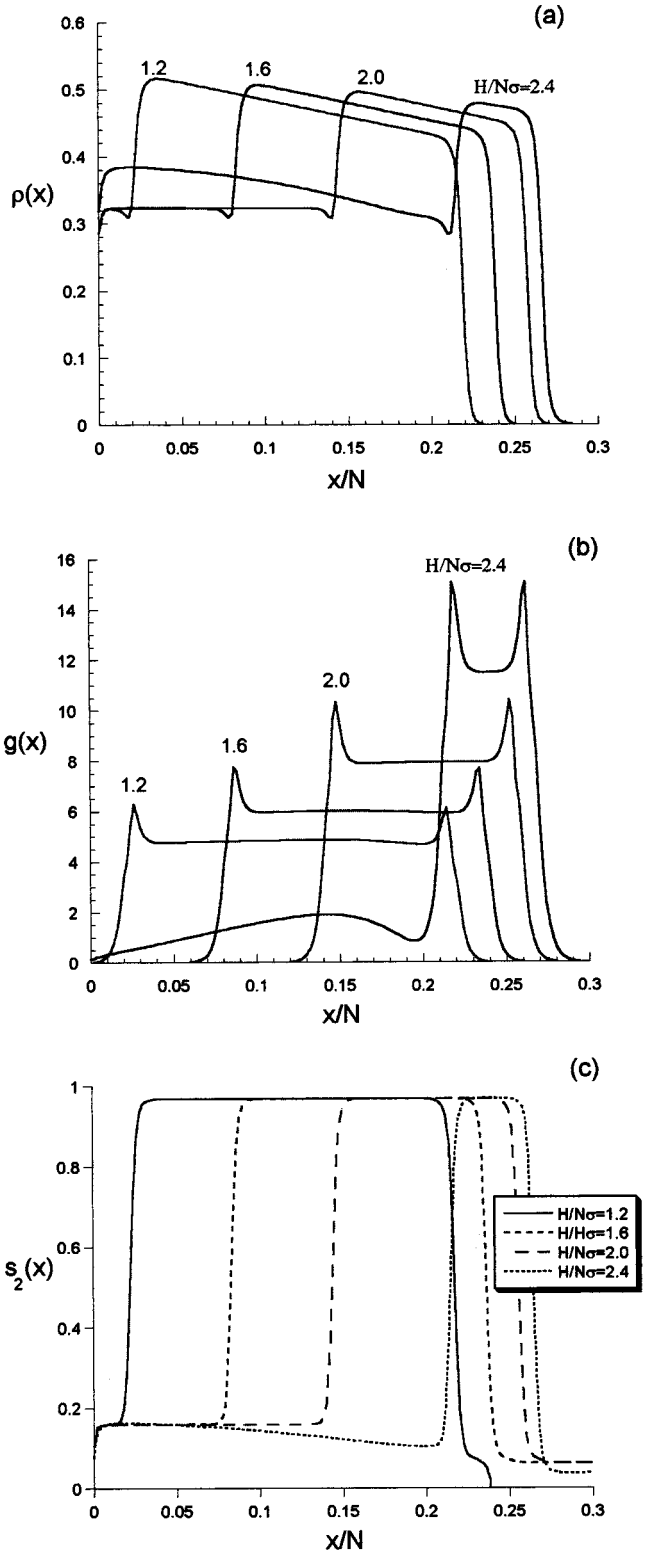

Figure 11. Evolution of density profiles (a), free end distribution (b), and orientational order parameter (c) with the stretching of combined FLC structure. The curves are obtained with successive increases in H from $H/N\sigma = 1.06$ to $H/N\sigma = 2.4$. $\sigma = 0.1$, $\chi = 0.25$, $\eta = 4.15$, $N = 500$, model (110).

is complementary to microphase separations due to the increase in anisotropic interactions and that due to the compression.[1−3]

The anisotropic interaction energy η affects the properties of sublayers of stretched chains. The greater is η, the lower is segment density in the stretched sublayers and the stronger is chain stretching s_1 (Figures 12 and 13). The value of η affects also the degree of stretching, limiting the existence of the GB system. If H is larger than a certain limiting value, which is the increasing function of η and is approximately equal to $H/N = s_1$, the stretched chains start escaping from the FLC sublayer. As shown in Figure 11 at $H/N\sigma = 2.4$, the FLC sublayer still exists, but some grafted chains do not reach this sublayer. These chains reside inside their own stretched sublayer and contribute to the density of segments there. Moreover, the density profile of the stretched sublayer is no longer constant and the shape of the density profile is similar to one for the CB brush. On a further increase in H the FLC sublayer disappears, and the GB brush−brush system breaks down into two separate CB brushes.

6. Equilibrium and Metastable States of Brushes

In the example investigated in the previous section, the brush−brush system breaks down into two separate brushes in the equilibrium CB state ($\eta = 4.15$). Analysis shows that the general behavior of glued FLC brushes in stretching and separating does not depend on η. In all cases, the brushes appear to be in the CB state after separation, although at large η, the true equilibrium state of a single brush is CB, MSB, or FLC depending on the value of η.

The diversity of states that can be reached at equivalent conditions shows that the minimization of the free energy in our numerical procedure can lead us not only to a global minimum but also to local minima. In other words, we are dealing not only with equilibrium but also with metastable states. For the sake of definiteness, let us analyze how the free energies of all the brush states observed in our system depend on H. Typical results are presented in Figure 14, referring to several values of the anisotropic interaction energy η, and hence corresponding to different equilibrium states of the undeformed single brush: CB state at $\eta = 4.15$, MSB state at $\eta = 4.3$, and FLC state at $\eta = 5.0$. These starting states are shown by stars in Figure 14a−c.

Parts a−c of Figure 14 illustrate the large diversity of stable and metastable states observed in our system. Each of these figures contains three different curves of the free energy as a function of H. Curve CB gives the free energy of interacting brushes preserving the CB state at all degrees of compression H. Curves CB hold practically the same position (except for the position of the left end) in Figure 14a−c, independent of the energy η of anisotropic interaction. This is due to the low degree of orientational order s_2 in CB brushes. (This "common" curve is shown by a dashed line in Figure 15.) The value of η affects, however, the position of curves MSB and GB referring to the interaction of partly (or totally) LC brushes. Curve MSB is the free energy of interacting MSB (or totally LC) brushes. Curve GB is the free energy of the combined FLC structure, i.e., the GB structure (equilibrium at small $H/N\sigma$ and stretched metastable at larger H).

The curves CB, MSB, and GB intersect each other. These intersection points are the points of first-order phase transitions from one structure to the other. The structure with minimal free energy at given H is the equilibrium one, the other structures at the same H are metastable ones. The type of equilibrium structure at a given H and the positions of the phase transition points depend on the value of η.

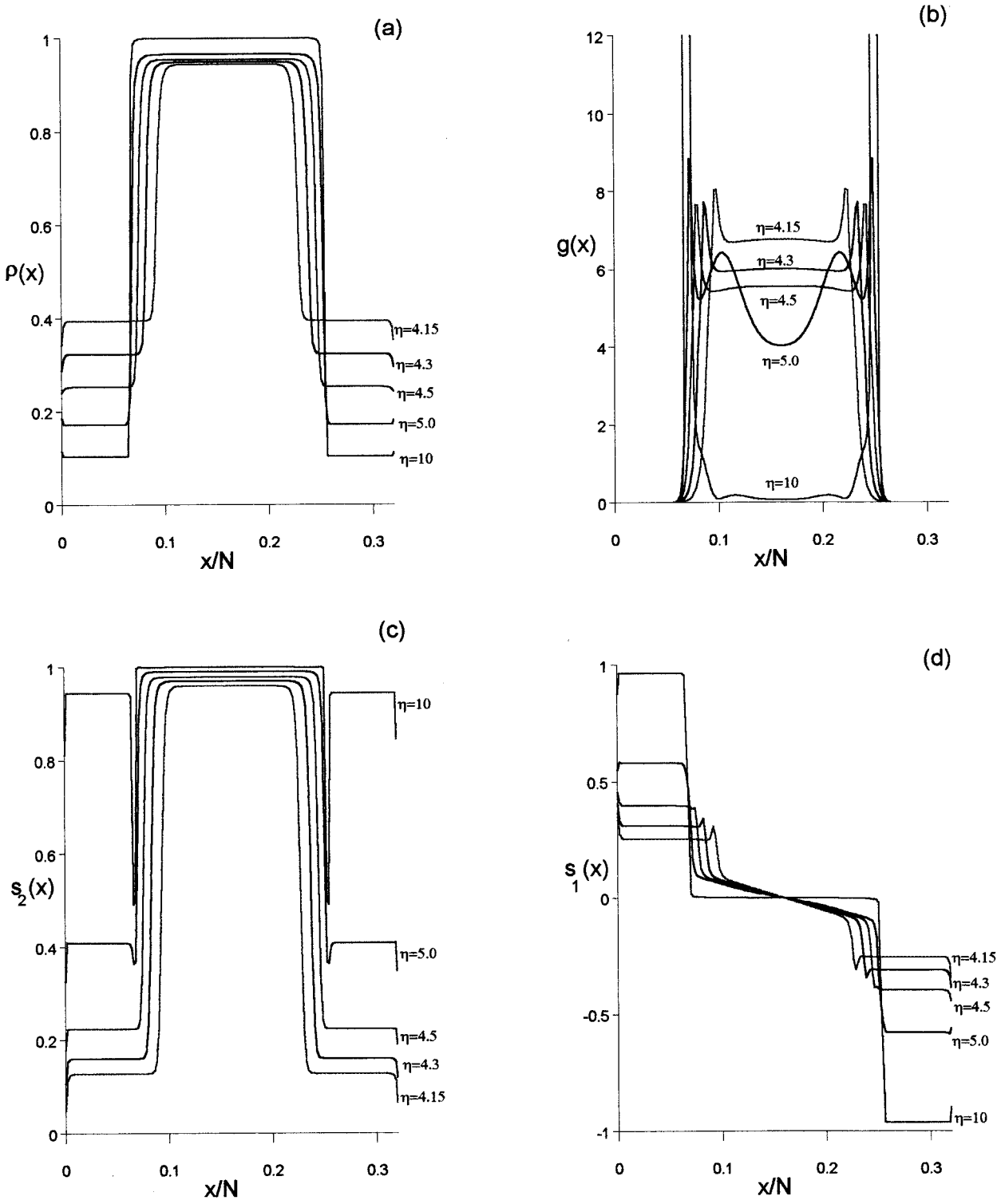

Figure 12. Characteristics of the stretched combined FLC structure $H/N\sigma = 1.6$ at different η: (a) density profiles; (b) free end distributions; (c) profiles of orientational order parameter s_2; (d) profiles of extension parameter s_1. $\sigma = 0.1$, $\chi = 0.25$, $N = 500$, model (110).

It must be emphasized that all curves in Figure 14 are obtained in our calculation as a result of a free energy minimization. This gives us ground to expect that we are dealing with global or local minima of the free energy, i.e., with stable or metastable states in our system. All curves are presented in intervals where the corresponding state was observed in our numerical procedure.

The different states at the same conditions are reached depending on the pathway, i.e., on the direction of variation of parameters in our calculations. It is possible to reason that these model results mimic the behavior of a real brush−brush system.

Let us follow the course of variation of the structure of a brush−brush system in the following sequence: single undeformed brush → compression → formation of the combined GB system → extension → breaking of the combined GB system into two single brushes.

At $\eta = 4.15$ single brushes are in the equilibrium CB state (Figure 14a). Compressed brushes preserve this

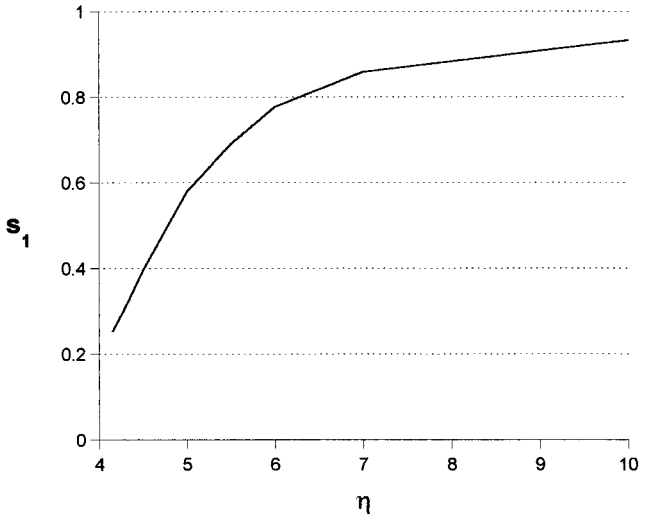

Figure 13. Degree of chain stretching s_1 in stretched sublayers vs the anisotropic interaction parameter η.

CB structure up to H corresponding to the point of intersection of curves CB and MSB. A first-order phase transition at the intersection point leads to a formation of MSB structure, which is an equilibrium one up to the MSB−GB intersection. In the interval of H between the CB−MSB and MSB−GB intersection the thickness of the internal LC sublayer increases with H. Near the MSB−GB intersection point each brush is practically completely in the FLC state. The first-order phase transition at the intersection point MSB−GB leads to a reconstruction of the individual FLC structures of each brush to form a combined GB structure of a brush−brush system as a whole. As can be seen from Figure 14a, this combined structure is an equilibrium one only within a narrow range of very strong compression near the limit $H/N\sigma = 1$. However, the brushes appear to be glued together. We observe a metastable stretched GB system under extension instead of the equilibrium MSB brushes. Only at large H do the brushes separate completely. Note that in all cases of intersection of different curves (including GB−CB intersection) we observe the effect of supercooling or superheating in intervals shown in Figure 14 (see also ref 1).

At larger η, in particular at $\eta = 4.3$ and $\eta = 5.0$ (Figure 14b,c), the equilibrium state of single brushes is the MSB or FLC state. The compression leads to the displacement of equilibrium from these states of brushes to the GB state of the combined system (first-order phase transition in the MSB−GB intersection point; see Figure 14b,c). At subsequent extension, this combined GB system of brushes glued together is a metastable one, and we observe it up to the value of H corresponding to the GB−CB intersection. At larger H, the combined structure breaks into two single brushes in the metastable CB state.

Hence after one compression−extension cycle our numerics give us the CB structure. At the next cycle of deformation, this CB state is preserved at an initial compression, and the mapping point is moving along the CB branch of the free energy curve (Figure 14) up to its left end point. Further compression leads to a transition to MSB and then GB states. The scenario of an extension is similar to that in the first cycle.

Figure 15 presents the curves $F(H)$ for the stretched combined GB structures at different η. All dependences

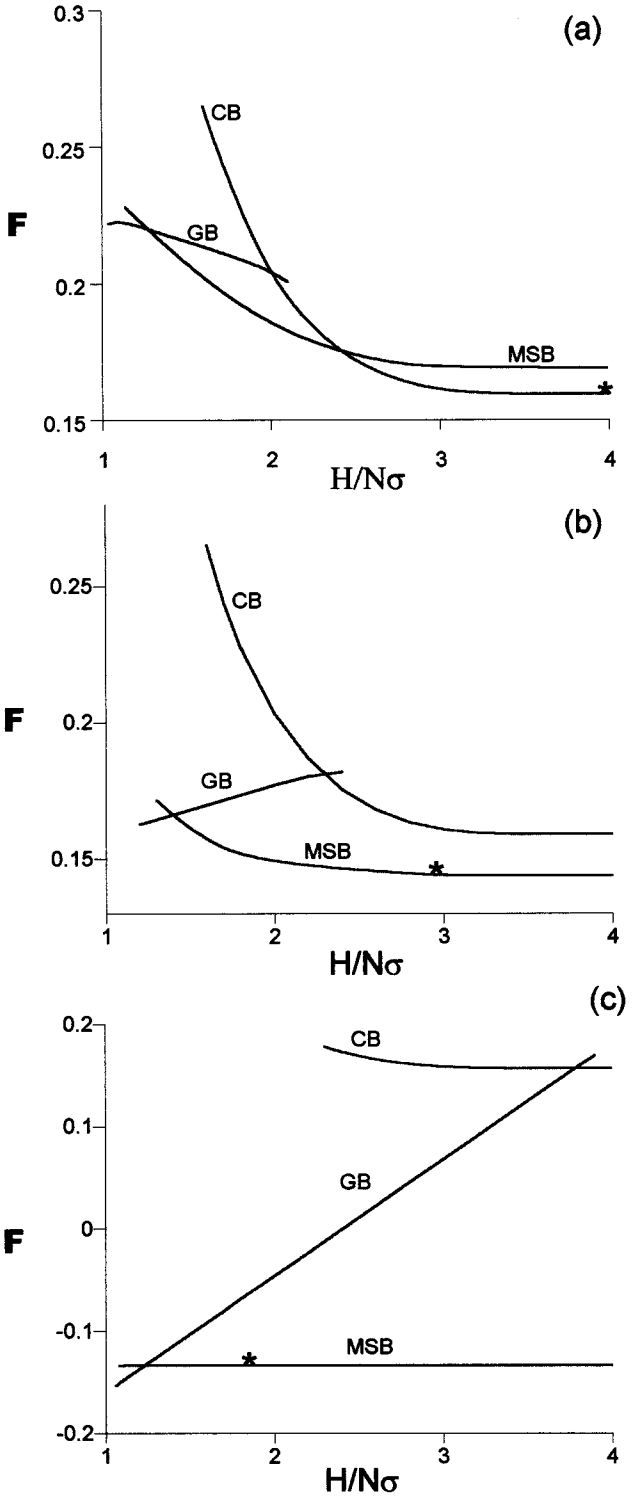

Figure 14. Free energies of segments as functions of the given value of H at different energies of anisotropic interaction: (a) $\eta = 4.15$; (b) $\eta = 4.3$; (c) $\eta = 5.0$. $\sigma = 0.1$, $\chi = 0.25$, $N = 500$, model (110). The asterisks show the starting states of an undeformed single brush.

are linear functions of H (with a small departure from linearity only near the right-hand end). This is typical for a two-phase system, in which the increase in H leads to redistribution of elements between two phases. In our case, these phases (microphases) are the stretched and the combined FLC sublayers. The dashed line gives the $F(H)$ curve for CB states, which is the same for all values of η.

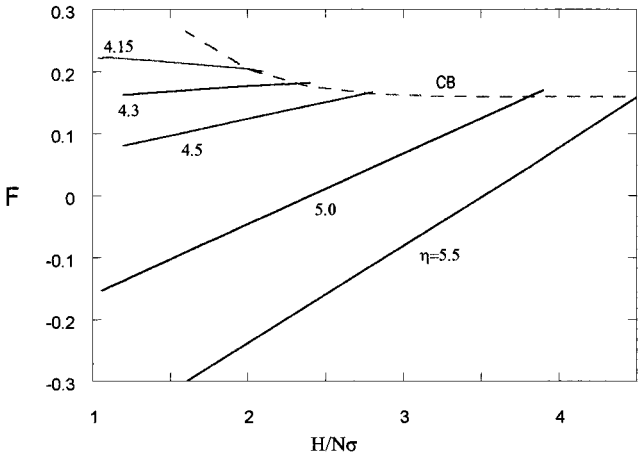

Figure 15. (Solid lines) free energies of combined GB structures for different energies η. (Dashed line) free energy of interacting CB brushes. (This curve is common for all η, except the position of a left end point: the lesser is η, the "longer" is the curve.)

7. Discussion

The numerical equilibrium SCF analysis in this and preceding papers[1−3] enables us to obtain a very rich picture of the behavior of polymer brushes formed by mesogenic chains. A number of different states are possible for such brushes, the transitions between them being first-order phase transitions. As is usual at first-order phase transitions, not only equilibrium but also metastable states can exist on each side of the transition. It is the combination of various stable and metastable states of the brushes that makes the picture so rich and leads to strong hysteresis effects.

In refs 1−3 (see also section 3 in this paper) we investigated and discussed the phase transition CB → MSB initiated by an increase in the relative value of the anisotropic interaction energy η or by the compression of the brush in the normal direction. In this paper we investigate the interaction of brushes oriented face-to-face under compression and subsequent extension. It is shown that the properties of such a system are unusual provided the chains in the brush acquire induced stiffness in the LC state.

The collapsed LC brush in this case is filled by long folds of grafted chains (FLC structure), and the contact between such brushes leads to interpenetration of brushes and to formation of a new equilibrium state (the combined GB structure) through the first-order phase transition. According to our calculations, the metastable state exists such that the system does not return to the initial state in an opposite process of extension of the combined GB structure. The brushes remain glued together. This metastable state is a two-phase state and contains the FLC structure in the central sublayer and the stretched structure in the two external sublayers.

Let us now try to answer two questions related to these results.

- Why do the FLC brushes form a combined GB structure?
- Why do the brushes appear to be glued together under extension of the initially compressed structure?

Roughly speaking, the LC brushes must satisfy two requirements: compactness of the brush and a high degree of orientational order, $\rho \simeq 1$ and $s_2 \simeq 1$. To satisfy $\rho \simeq 1$, it is necessary to fold each chain in a brush. To satisfy $s_2 \simeq 1$, it is necessary to minimize the number of folds. Really, each change of direction of 180° in the case of chain with induced rigidity ($\alpha_b = 0$) produces an additional segment oriented unfavorably. The same effect leads to interpenetration of contacting FLC brushes. Formation of a combined GB structure leads to a decrease in the number of folds in each brush.

The fact that according to our calculations the brushes do not separate under moderate extension suggests that the barrier between this local minimum and the global minimum is rather high. Unfortunately, the SCF method does not allow us to analyze the kinetic aspects of the transitions (the height of barriers, the times of transitions between different states, etc.). We only can point out that the process of "moving" a GB system under extension is similar to going up a "mountain serpentine"; i.e., it is necessary to push grafting planes by small increases in H. Too high an increase in H results in destruction of the metastable combined GB system.

In conclusion, it is reasonable to suggest that our picture of a large number of stable and metastable states may be true not only for the model system but also for real FLC brushes. This might lead to some very interesting properties.

Acknowledgment. The authors express their gratitude to L. I. Klushin for helpful discussion. We acknowledge the Russian Foundation for Basic Research (grants 96-03-33862 and 96-1597401) and Russian Federal Program "Integration" (grant 326.38) for financial support.

References and Notes

(1) Amoskov, V. M.; Birshtein, T. M.; Pryamitsyn, V. A. *Macromolecules* **1996**, *29*, 7240.
(2) Mercurieva, A. A.; Birshtein, T. M.; Pryamitsyn, V. A.; Polotskij, A. *Macromol. Chem., Theory Simul.* **1996**, *5*, 215.
(3) Birshtein, T. M.; Amoskov, V. M.; Mercurieva, A. A.; Pryamitsyn, V. A. *Macromol. Symp.* **1997**, *113*, 151.
(4) Milner, S. T. *Science* **1991**, *251*, 905.
(5) Zhulina, E. B.; Borisov, O. V.; Pryamitsyn, V. A. *J. Colloid Interface Sci.* **1990**, *137* (2), 590.
(6) Flory, P. J. *Principles of Polymer Chemistry*; Cornell University: Ithaca, NY, 1953.
(7) DeGennes, P.-G. *Scaling Concepts in Polymer Physics*; Cornell University Press: Ithaca, NY, 1979.
(8) Maier, W.; Saupe, A. *Z. Naturforsch. A* **1959**, *14*, 10, 882.
(9) Scheutjens, J. M.; Fleer, G. J. *J. Phys. Chem.* **1979**, *83*, 1619.
(10) Zhulina, E. B.; Pryamitsyn, V. A.; Borisov, O. V. *Polym. Sci. USSR* **1989**, *30*, 205.
(11) Milner, S. T.; Witten, T. A.; Cates, M. E. *Macromolecules* **1988**, *21*, 2610.
(12) Zhulina, E. B.; Borisov, O. V.; Pryamitsyn, V. A.; Birshtein, T. M. *Macromolecules* **1991**, *24*, 140.
(13) Wijmans, C. M.; Leermakers, F. A. M.; Fleer, G. J. *J. Chem. Phys.* **1994**, *101*, 8214.
(14) Halperin, A.; Zhulina, E. B. *Macromolecules* **1991**, *24*, 5393.
(15) Zhulina, E. B.; Halperin, A. *Macromolecules* **1992**, *25*, 5730.
(16) Zhulina, E. B.; Birshtein, T. M.; Pryamitsyn, V. A.; Klushin, L. I. *Macromolecules* **1995**, *28*, 8612.

MA970985D